



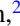













Reduction of spectroscopic overlap across the $Z = 8$ shell in neutron-rich nuclei

T. Redpath ^{1,2,*} P. Guèye ^{1,3,†} T. Baumann ¹ B. A. Brown ¹ A. Cunningham ^{2,‡} P. A. DeYoung ⁴ N. Frank ⁵
 C. R. Hoffman ⁶ A. N. Kuchera ⁷ B. Monteagudo Godoy ⁴ C. Persch ^{4,§} A. Revel ^{1,3} W. F. Rogers ⁸
 M. Thoennessen ^{1,3} J. A. Tostevin ⁹ and D. Votaw ^{1,3,||}

¹Facility for Rare Isotope Beams, Michigan State University, East Lansing, Michigan 48824, USA

²Department of Chemistry, Virginia State University, Petersburg, Virginia 23806, USA

³Department of Physics and Astronomy, Michigan State University, East Lansing, Michigan 48824, USA

⁴Department of Physics, Hope College, Holland, Michigan 49422-9000, USA

⁵Department of Physics, Engineering, and Astronomy, Augustana College, Rock Island, Illinois 61201, USA

⁶Physics Division, Argonne National Laboratory, Lemont, Illinois 60439, USA

⁷Department of Physics, Davidson College, Davidson, North Carolina 28035, USA

⁸Department of Physics, Indiana Wesleyan University, Marion, Indiana 46953, USA

⁹Department of Physics, University of Surrey, Guildford GU2 7XH, United Kingdom



(Received 9 March 2024; accepted 25 April 2024; published 24 May 2024)

Background: The recent discovery and spectroscopic measurements of ^{27}O and ^{28}O suggests the disappearance of the $N = 20$ shell structure in these neutron-rich oxygen isotopes.

Purpose: We measured one- and two-proton removal cross sections from ^{27}F and ^{29}Ne , respectively, extracting spectroscopic factors and comparing them to shell model overlap functions coupled with eikonal reaction model calculations.

Method: The invariant mass technique was used to reconstruct the two-body ($^{24}\text{O} + n$) and three-body ($^{24}\text{O} + 2n$) decay energies from knockout reactions of ^{27}F (106.2 MeV/u) and ^{29}Ne (112.8 MeV/u) beams impinging on a ^9Be target.

Results: The one-proton removal from ^{27}F strongly populated the ground state of ^{26}O and the extracted cross section of $3.4_{-1.5}^{+0.3}$ mb agrees with eikonal model calculations that are normalized by the shell model spectroscopic factors and account for the systematic reduction factor observed for single nucleon removal reactions within the models used. For the two-proton removal reaction from ^{29}Ne an upper limit of 0.08 mb was extracted for populating states in ^{27}O decaying through the ground state of ^{26}O .

Conclusions: The measured upper limit for the population of the ground state of ^{26}O in the two-proton removal reaction from ^{29}Ne indicates a significant difference in the underlying nuclear structure of ^{27}F and ^{29}Ne .

DOI: [10.1103/PhysRevC.109.054325](https://doi.org/10.1103/PhysRevC.109.054325)

I. INTRODUCTION

More than 25 years after the first unsuccessful search for ^{28}O [1] and its independent confirmation in 1999 [2], unbound ^{28}O decaying into ^{24}O and four neutrons was finally discovered [3]. The observation of a narrow resonance at

$460_{-40}^{+50}(\text{stat}) \pm 20(\text{syst})$ keV which most likely corresponds to the ground state confirms that ^{24}O is the last bound oxygen isotope and thus defines the location of the dripline in oxygen at ^{24}O . In contrast, the last bound fluorine isotope has been determined to be ^{31}F [2,4] and one of the major outstanding questions has been how the addition of one proton can bind six additional neutrons. Only recently have theoretical calculations been able to reproduce this phenomenon [3,5], but a consistent description of the spectroscopy in this region has still not been achieved. It is interesting to note that the current Atomic Mass Evaluation still extrapolates ^{31}F to be unbound with respect to two-neutron emission by 500 ± 100 keV [6].

The difficulties in reproducing the experimental observations in this mass region are due to the disappearance of the $N = 20$ shell gap and the related existence of the island of inversion where intruder states of the pf shell fall below the sd -shell levels [7]. The measured single proton removal cross section from ^{29}F populating ^{28}O indicates the influence of the island of inversion beyond fluorine into the oxygen isotopes [3]. Other recent experiments helped delineate the southern

*tredpath@vsu.edu

†gueye@frib.msu.edu

‡Present address: Morehouse School of Medicine, Atlanta, GA 30310, USA.

§Present address: Department of Atmospheric and Oceanic Sciences, University of Colorado, Boulder, CO 80309, USA.

||Present address: U.S. Department of Defense, Washington, DC 20301, USA.

Published by the American Physical Society under the terms of the [Creative Commons Attribution 4.0 International](https://creativecommons.org/licenses/by/4.0/) license. Further distribution of this work must maintain attribution to the author(s) and the published article's title, journal citation, and DOI.

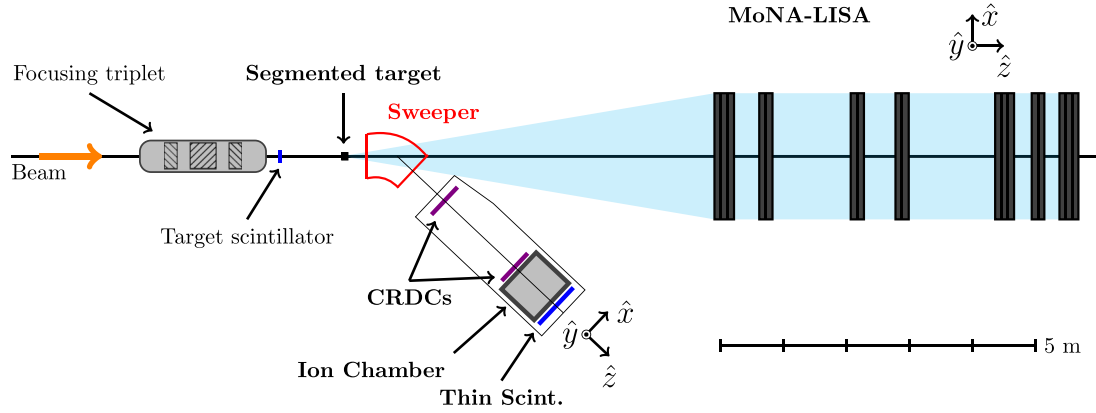


FIG. 1. Overview of the experimental setup [30].

border of the island of inversion. In neutron-rich neon isotopes the emergence of low-lying intruder states was observed [8–13] and the boundary of the island of inversion was located at ^{28}Ne [9,14] with positive and negative parity ground states in ^{27}Ne [15] and ^{29}Ne [16,17], respectively. In fluorine, the transition into the island of inversion has been determined to occur between ^{27}F and ^{28}F [18–20].

If and how strongly the island of inversion reaches into the oxygen isotopes can be studied by measuring the spectroscopic overlap of neutron-rich oxygen isotopes with fluorine and neon isotopes in one-proton and two-proton removal reactions. For example, in a recent measurement of the one-proton removal reaction from the $5/2^+$ ground state of ^{25}F populating ^{24}O , a significant reduction of the $d_{5/2}$ strength relative to shell-model calculations was observed [21,22]. In order to extend these types of measurements to even more neutron-rich oxygen isotopes we studied one- and two-proton removal reactions from ^{27}F and ^{29}Ne , respectively.

As mentioned above, the ground state of ^{27}F is located outside of the island of inversion with a ground state spin and parity $5/2^+$, while the ground state of ^{29}Ne is $3/2^-$ and thus lies within the island of inversion. ^{26}O was determined to be unbound in 1990 [23] and it took more than 20 years to measure its two-neutron decay to ^{24}O [24–26]. Subsequently, a higher precision value for the decay energy [$18 \pm 3(\text{stat}) \pm 4(\text{syst})$ keV] as well as the first excited 2^+ ($1.28_{-0.08}^{+0.11}$ MeV above threshold) were reported [27]. ^{27}O was only discovered recently in the decay of ^{28}O following the single proton removal of ^{29}F [3]. A state at a decay energy of $1.09 \pm 0.04(\text{stat}) \pm 0.02(\text{syst})$ MeV relative to ^{24}O was observed. In addition, a few events consistent with this observation were also identified in the reaction $^{29}\text{Ne}(-2p)^{27}\text{O}$, which is the same reaction reported in the present paper.

II. EXPERIMENTAL METHOD AND DATA

This experiment was conducted at the National Superconducting Cyclotron Laboratory located on the campus of Michigan State University. Secondary beams of 106.2 MeV/u ^{27}F and 112.8 MeV/u ^{29}Ne were produced simultaneously from a 140 MeV/u ^{48}Ca primary beam that impinged on a 775 mg/cm^2 beryllium production target at the Coupled Cyclotron Facility [28]. ^{27}F and ^{29}Ne fragments were identified

and separated with the A1900 fragment separator [29] and transmitted to the MoNA-LISA/Sweeper experimental area. Both beams impinged on a Be-Si segmented target that consisted of a stack of three ^9Be targets with thicknesses of 3.3 mm, 3.7 mm, and 4.1 mm, respectively, sandwiched between four $140 \mu\text{m}$ thick silicon detectors [30]. Neutron-unbound oxygen isotopes were populated in one-proton and two-proton removal reactions from the ^{27}F and ^{29}Ne beams, respectively. These isotopes decayed within the target by neutron emission to the heaviest bound oxygen isotope, ^{24}O . The ^{24}O fragments were deflected toward the charged particle detector suite through a large-gap Sweeper magnet [31] set at a rigidity of 3.445 Tm. The emitted neutrons were detected by the MoNA-LISA neutron array [32]. Figure 1 shows the experimental setup and further details can be found in Refs. [30,33].

Incident beam particles (^{27}F or ^{29}Ne) were within the acceptance of the Sweeper magnet. The atomic numbers (Z) for unreacted beam and reaction products from the segmented target were identified by measuring the time of flight (ToF) between the target and thin scintillators and the energy loss in the ionization chamber.

Mass (A) identification was achieved by correcting the raw ToF for position and angle after the Sweeper magnet, as well as for the position of the incoming beam measured by the first silicon detector of the segmented target. These corrections are made to approximately compensate for the energy spread of the reaction fragments and path length differences in their trajectories through the Sweeper magnetic field. Two cathode readout drift chambers (CRDCs) measured the positions of the fragments at two points after the Sweeper (see Fig. 1) to provide position and angle information at the final thin scintillator. Unfortunately, the first CRDC experienced an uncorrectable hardware failure that corrupted its position information in specific regions across its active area. As a result, the aforementioned ToF corrections could only be extracted for regions of the emittance with viable CRDC1 position information, limiting the efficiency to 40%. This was determined from the ratio of $Z = 8$ events inside the viable emittance regions divided by the total number of $Z = 8$ events. This 40% value is the same for both beams since both ^{27}F and ^{29}Ne and their reaction products filled similar regions of the acceptance. Further details can be found in Ref. [33].

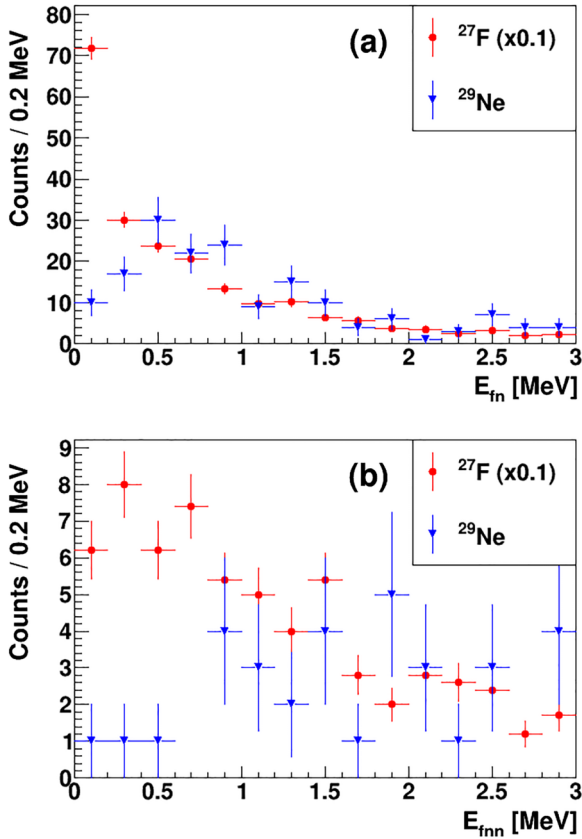


FIG. 2. Reconstructed $^{24}\text{O}+n$ two-body (top) and $^{24}\text{O}+2n$ three-body (bottom) decay energy spectra from ^{27}F (red, scaled by 0.1) and ^{29}Ne (blue) beams. The three-body data were filtered using the conditions described in the text.

The reconstructed two-body decay energies were obtained from the coincidence between the ^{24}O fragment and the first neutron interaction in the MoNA-LISA detector array and are shown in Fig. 2(a). While the distribution from ^{27}F (red) shows clear evidence for the ^{26}O ground state at very low decay energies, such a contribution is absent or highly suppressed for ^{29}Ne (blue).

This observation is confirmed in the three-body spectra which were reconstructed from coincidences between ^{24}O and the first two neutrons. Each emitted neutron can potentially interact multiple times within subsequent bars of MoNA-LISA. In order to calculate the correct three-body decay energy for each event, the following procedure was implemented to suppress the contribution from events in which one neutron is detected multiple times. First, the spatial and time separation between all recorded neutron interactions in an event are checked and clusters are formed from interactions within 20 cm and 3.5 ns of one another. For each cluster, the earliest hit is taken as the initial neutron interaction and the remaining hits associated with the cluster are discarded, thus reducing the cluster to a single hit. Next, the neutron interactions from all cluster reductions are checked pair-wise for causal connections. Two interactions are considered to be causally connected if they satisfy $v_b^2 dt^2 - s^2 > -300 \text{ cm}^2$ and $\theta < 80^\circ$, where v_b is the beam velocity, dt is the time

difference between two interactions, s is the spatial separation between interactions, and θ is the angle between the vector that points from the target to the earlier hit and the vector that connects the two interactions. The quoted limits were chosen to balance multi-interaction rejection and two-neutron detection efficiency. Interactions found to be causally connected could be capturing two hits by the same neutron. In this case, the second interaction is discarded. Only events with two or more hits remaining after this filtering process are included in the final three-body decay energy spectra shown in Fig. 2(b).

III. SIMULATIONS AND RESULTS

In order to interpret the experimental spectra, a detailed Monte Carlo simulation [34,35] was used to produce simulated data sets that take into account the locations and dimensions of the target and the detectors as well as the beam profile, reaction and decay processes, energy losses in the segmented target, and neutron interactions in MoNA-LISA.

The population and possible decay paths included in the simulations are shown in Fig. 3. The decay parameters for ^{25}O ($E = 749 \text{ keV}$, $\Gamma = 88 \text{ keV}$) and the decay energies of the ^{26}O 0^+ ground state (18 keV) and first excited 2^+ state (1.28 MeV) were taken from Ref. [27]. The width of the 2^+ state (270 keV) was taken from Ref. [36]. In addition to these discrete known states, the simulations for the ^{27}F induced reactions included the population of a broad, highly excited continuum in ^{26}O , which could be populated by removing a p -shell proton. The second 0^+ state in ^{26}O has not been observed yet and is not expected to be populated by one-proton removal from ^{27}F .

For the ^{29}Ne induced reactions, the statistics were not sufficient to generate four-body ($^{24}\text{O} + 3n$) spectra. However, the lack of low-energy strength in the three-body, as well as the two-body, data show that the decay path through the ^{26}O ground state is strongly suppressed. Thus the focus of the simulations was on establishing a limit for this path as it would yield significant constraints on the location and population of low lying states in ^{27}O . Therefore, the simulations only included the population and decay of the ^{26}O 0^+ ground and the first excited 2^+ states.

The events generated by the simulations were filtered with the same gates and conditions as the data. Specifically, for the three-body ($^{24}\text{O} + 2n$) spectra the causality gates were applied. With these boundary conditions, fits to the data were performed where only the overall cross sections and the relative contributions of the populated states were free parameters. For the ^{27}F reaction the relative contributions of the 2^+ and the higher lying states were not well defined, so the relative population of the 2^+ to the 0^+ was extracted from Refs. [27,37] to be 23–30 % and 77–70 %, respectively.

The results of the final fits are shown in Fig. 4. In the ^{27}F reaction the final extracted cross sections were $3.4^{+0.3}_{-1.5} \text{ mb}$ and $1.4^{+0.2}_{-0.6} \text{ mb}$ for the 0^+ and 2^+ , respectively. For the ^{29}Ne reaction an upper limit of 0.08 mb for 0^+ state and 0.9(2) mb for populating the 2^+ state were extracted.

As the data were recorded in fragment singles mode, we can also extract the integrated cross section populating the ground state of ^{24}O . After subtracting the contributions from

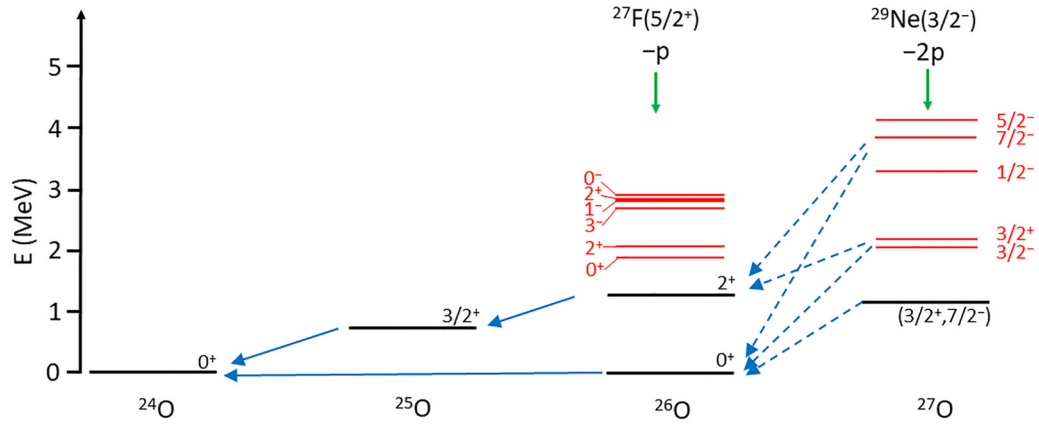


FIG. 3. Level scheme of the neutron-unbound oxygen isotopes populated in the present reactions. Experimentally known states for $^{24-27}\text{O}$ are shown in black. The energies and spin and parity assignments for $^{25-26}\text{O}$ were taken from Ref. [27] while the energy and tentative spin and parity assignments for ^{27}O are from Ref. [3]. States in ^{26}O and ^{27}O predicted by shell model calculations are shown in red. Decay paths included in the simulations are indicated by solid blue arrows. The dashed blue arrows show possible decays of states populated in ^{27}O (see Sec. IV for details.)

the 0^+ and 2^+ states the measured value of 17.6 mb for the ^{27}F induced reaction corresponds to about 13 mb decaying to ^{24}O via highly excited states in ^{26}O . This value is consistent with measurements in the lighter fluorine isotopes $^{24-26}\text{F}$ [38]. These states are primarily populated by proton removal from the p shell [38,39]. The integrated cross section for populating ^{24}O from the ^{29}Ne was about 3 mb.

IV. COMPARISON WITH THEORY

We performed shell model calculations with the FSU *spdfp* cross shell interaction [40] to compute the spectroscopic occupancies for the initial and final nuclei for the

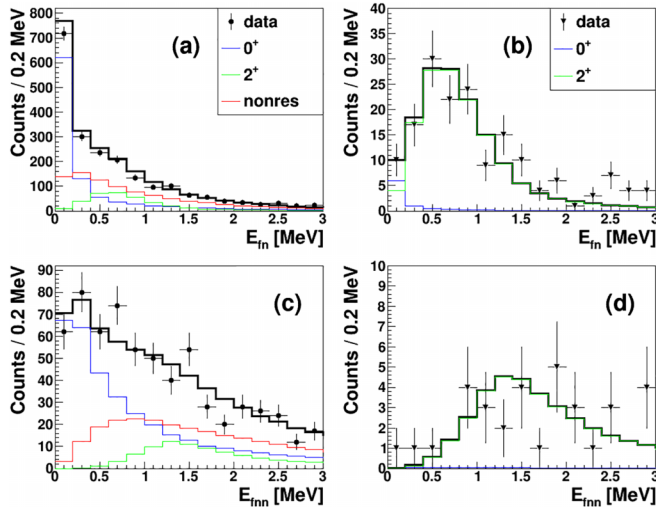


FIG. 4. Top panel: reconstructed two-body decay energy ($^{24}\text{O} + n$) from ^{27}F (a) and ^{29}Ne (b) incident beams on the segmented beryllium target. Bottom panel: reconstructed three-body decay energy ($^{24}\text{O} + 2n$) from ^{27}F (c) and ^{29}Ne (d) incident beams on a beryllium target. The results of the simulations are shown in black solid lines which are the sums of the individual decay contributions indicated as solid colored lines in the panels and discussed in the text.

present reactions. The calculated low-lying levels for ^{26}O and ^{27}O are shown in red in Fig. 3. It should be noted that the FSU Hamiltonian can only be used to calculate the energies of the pure $n\hbar\omega$ configurations [41] and that some of the energies in Fig. 3 need to be shifted down by about 0.8 MeV to agree with known data.

The configurations of the shell model states were used to calculate one- and two-proton removal cross sections with the eikonal direct-reaction model for the ^{27}F [42] and ^{29}Ne [43] induced reactions, respectively. The ground state of ^{27}F has spin and parity of $5/2^+$ [18] with the valence proton occupying the $\pi d_{5/2}$ orbital. The spectroscopic factors (C^2S) for the removal of this proton, single-particle cross sections (σ_{sp}), and the cross sections from the eikonal model (σ_{eikonal}) are listed in Table I for populating the ground and first excited states of ^{26}O . The eikonal model cross sections are obtained from the product of the center of mass correction, the spectroscopic factor, and the single-particle cross section: $\sigma_{\text{eikonal}} = [A/(A-1)]^N (C^2S) \sigma_{\text{sp}}$, where N is the number of oscillator quanta of the orbital from which the nucleon is removed; here $N = 2$.

For single proton removal reactions the systematics of the eikonal model predictions for numerous systems are that the cross sections have to be further reduced by a factor R_s which depends on the difference of the proton and neutron

TABLE I. Calculated spectroscopic factors (C^2S) for the removal of the valence $\pi d_{5/2}$ proton and single-particle (σ_{sp}), eikonal model (σ_{eikonal}), theoretical (σ_{theo}), and experimental (σ_{exp}) cross sections (in mb) for the one-proton removal reaction from the ^{27}F $5/2^+$ ground state populating the ground state and first excited state (J^π) in ^{26}O .

J^π	C^2S	σ_{sp}	σ_{eikonal}	σ_{theo}	σ_{exp}
0^+	0.84	13.73	12.41	4.6 ± 1.9	$3.4^{+0.3}_{-1.5}$
2^+	0.14	12.97	2.13 ^a	0.7 ± 0.3	$1.4^{+0.2}_{-0.6}$

^aThis value includes contributions from small admixtures of 0.001 and 0.01 from $d_{3/2}$ and $s_{1/2}$, respectively.

ground-state separation energies ($\Delta S = S_p - S_n$) [44]. For the present reaction ΔS is 15.2 MeV, yielding an R_s value of 0.37(15). The final calculated theoretical cross sections (σ_{theo}) are consistent within the uncertainties with the measured cross sections (σ_{exp}).

For the two-proton removal reaction from ^{29}Ne , only very few events for the decay paths of ^{27}O via the ground state of ^{26}O were observed and an upper limit of 0.08 mb was extracted. This result is consistent with the recent observation of states in ^{27}O [3]. In the reaction $^{29}\text{F}(-1p)^{28}\text{O}$, a state in ^{27}O at a decay energy of 1.09 MeV was tentatively assigned to be $3/2^+$ or $7/2^-$. However, this reaction could also result in the population of a $3/2^-$ state dependent upon the $0\hbar\omega$ - $2\hbar\omega$ mixing in the ^{29}F ground state. A state at about 1 MeV observed in the reaction $^{29}\text{Ne}(-2p)^{27}\text{O}$ was “consistent with the sequential decay of the ^{27}O resonance observed in the ^{29}F beam data” as mentioned by Kondo *et al.* [3]. It should be noted that the data shown in Ref. [3] were gated on a low-energy neutron, thus enhancing the contribution of decays through the ^{26}O ground state. Kondo *et al.* did not extract a cross section for the ^{29}Ne reaction. However, they state that “the cross section for the two-proton removal was much lower than expected” [3].

The ground state of ^{29}Ne has negative parity [16,17], so that positive parity states in the two-proton removal reaction can only be populated by the removal of a p -shell proton which most likely will result in the population of highly excited states, however, a (very) small admixture to the first excited $3/2^+$ cannot be excluded. Thus, the observed states by Kondo *et al.* in the ^{29}Ne and ^{29}F induced reactions are either the same state ($7/2^-$, $3/2^+$, or $3/2^-$), or the state observed with the ^{29}F beam is essentially degenerate with a $3/2^-$ state populated with the ^{29}Ne beam.

Let us first consider the scenario where a low-lying $3/2^-$ level in ^{27}O is populated in the $^{29}\text{Ne}(-2p)$ reaction. SDPF-M large-scale shell model calculations have computed that the $3/2^-$ state in ^{29}Ne consists of 66.4% $3\hbar\omega$ and 32.4% $1\hbar\omega$ configurations due to the onset of deformation [16]. The two-proton removal reaction from the $3\hbar\omega$ component in ^{29}Ne would lead to $3\hbar\omega$ excited states in ^{27}O that cannot decay to the low-lying $0\hbar\omega$ 0^+ and 2^+ states in ^{26}O . For a pure $1\hbar\omega$ configuration in ^{29}Ne the eikonal reaction model calculates two-proton removal cross sections of 0.57 mb and 0.12 mb to the $1\hbar\omega$ $3/2^-$ and $7/2^-$ states in ^{27}O , respectively. Assuming 32.4% $1\hbar\omega$ configurations in ^{29}Ne , the cross sections to the $3/2^-$ state would be 0.18 mb. In the FSU *spsdfp* cross shell interaction the $3/2^-$ state is described as ^{26}O plus a valence neutron [$\nu 1(p_{3/2})$] and would thus be very broad (~ 700 keV). The observed limit of 0.08 mb for the decay of ^{27}O to the ^{26}O ground state means that less than a half of the broad $3/2^-$ state decays to the ^{26}O ground state or that the percentage of $1\hbar\omega$ in ^{29}Ne is less than 15%.

A $3/2^+$ ground state of ^{27}O has been predicted by Gamow shell model (GSM) calculations using the density matrix renormalization group (DMRG) method [36] where the $3/2^+$ ground state is less than an MeV above the $^{26}\text{O}+n$ ground state and the $3/2^-$ at an excitation energy of more than 5 MeV [45]. However, as mentioned before, the population of a $3/2^+$ state from the $3/2^-$ ground state of ^{29}Ne by two

proton removal is extremely unlikely. It also would represent a complete structural change between these two nuclides.

Similarly, the assignment of a spin and parity of $7/2^-$ is improbable. It would correspond to a reversal of the level ordering from ^{29}Ne . Although $f_{7/2}$ components in the ground state of ^{29}Ne have been reported, it is dominated by p -wave strength ($p_{3/2}$) [13,16]. These configurations persist in ^{28}F where the $p_{3/2}$ also dominates the ground state [17]. Thus, a $7/2^-$ ground state in ^{27}O would represent a significant structural change across the $Z = 8$ shell. Such a level reversal and structural change has not been predicted by any of the current theoretical models.

In all these scenarios, the structural overlap between the ^{29}Ne ground state and the lowest lying $3/2^-$ state in ^{27}O is significantly smaller than predicted by the shell model calculations. This mismatch of the configurations could be due to either of these two nuclei.

A similar overlap mismatch has also recently been reported in the proton removal from ^{25}F populating ^{24}O [22]. In contrast, in the recent discovery of ^{28}O in the $(p, 2p)$ reaction from ^{29}F the measured cross section was consistent with similar neutron configurations in ^{29}F and ^{28}O [3].

V. SUMMARY AND CONCLUSION

One- and two-proton removal reactions from ^{27}F and ^{29}Ne , respectively, were measured and the two-body ($^{24}\text{O}+n$) and three-body ($^{24}\text{O}+2n$) decay energy spectra were reconstructed. The extracted cross sections for populating the ground- and the first-excited state in ^{26}O from the reaction $^{27}\text{F}(-p)$ were $3.4^{+0.3}_{-1.5}$ mb and $1.4^{+0.2}_{-0.6}$ mb, respectively. In the two-proton removal reaction from ^{29}Ne the decay via the ground state of ^{26}O was strongly suppressed and only an upper limit of <0.08 mb was extracted. This observation indicates a small configuration overlap between ^{29}Ne and ^{27}O and represents a challenge for a consistent description of the structure of these neutron-rich nuclei across the $Z = 8$ shell.

ACKNOWLEDGMENTS

This experiment was performed at the NSF’s National Superconducting Cyclotron Laboratory (NSCL). The expertise of NSCL operations staff and of the A1900 separator group is gratefully acknowledged. This work was supported by the National Science Foundation under Grants No. PHY-1565546, No. PHY-2012040, No. PHY-2110365 (MSU), No. PHY-1613188 (Hope College), No. PHY-1713522 (Augustana College), No. PHY-2011398 (Davidson College), and No. EES-2100969 (Virginia State University). This work was also based upon work supported by the Department of Energy National Nuclear Security Administration through the Nuclear Science and Security Consortium under Award No. DE-NA0003180 and by the U.S. Department of Energy, Office of Science, Office of Nuclear Physics, under Grant No. DE-SC0022075 (MSU) and Contract No. DE-AC02-06CH11357 (Argonne). J.A.T. acknowledges support from the Science and Technology Facilities Council (U.K.) Grant No. ST/V001108/1. We would like to thank Profs. Kondo-san, Nakamura-san, and Kevin Fosse for fruitful discussions.

- [1] O. Tarasov, R. Allatt, J. C. Angélique, R. Anne, C. Borcea, Z. Dlouhy, C. Donzaud, S. Grévy, D. Guillemaud-Mueller, M. Lewitowicz, S. Lukyanov, A. C. Mueller, F. Nowacki, Y. Oganessian, N. A. Orr, A. N. Ostrowski, R. D. Page, Y. Penionzhkevich, F. Pougheon, A. Reed *et al.*, *Phys. Lett. B* **409**, 64 (1997).
- [2] H. Sakurai, S. M. Lukyanov, M. Notani, N. Aoi, D. Beaumel, N. Fukuda, M. Hirai, E. Ideguchi, N. Imai, M. Ishihara, H. Iwasaki, T. Kubo, K. Kusaka, H. Kumagai, T. Nakamura, H. Ogawa, Y. E. Penionzhkevich, T. Teranishi, Y. X. Watanabe, K. Yoneda *et al.*, *Phys. Lett. B* **448**, 180 (1999).
- [3] Y. Kondo, N. L. Achouri, H. Al Falou, L. Atar, T. Aumann, H. Baba, K. Boretzky, C. Caesar, D. Calvet, H. Chae, N. Chiga, A. Corsi, F. Delaunay, A. Delbart, Q. Deshayes, Z. Dombrádi, C. A. Douma, A. Ekström, Z. Elekes, C. Forssén *et al.*, *Nature (London)* **620**, 965 (2023).
- [4] D. S. Ahn, N. Fukuda, H. Geissel, N. Inabe, N. Iwasa, T. Kubo, K. Kusaka, D. J. Morrissey, D. Murai, T. Nakamura, M. Ohtake, H. Otsu, H. Sato, B. M. Sherrill, Y. Shimizu, H. Suzuki, H. Takeda, O. B. Tarasov, H. Ueno, Y. Yanagisawa *et al.*, *Phys. Rev. Lett.* **123**, 212501 (2019).
- [5] N. Tsunoda, T. Otsuka, K. Takayanagi, N. Shimizu, T. Suzuki, Y. Utsuno, S. Yoshida, and H. Ueno, *Nature (London)* **587**, 66 (2020).
- [6] M. Wang, W. J. Huang, F. G. Kondev, G. Audi, and S. Naimi, *Chin. Phys. C* **45**, 030003 (2021).
- [7] E. K. Warburton, J. A. Becker, and B. A. Brown, *Phys. Rev. C* **41**, 1147 (1990).
- [8] Z. Dombradi, Z. Elekes, A. Saito, N. Aoi, H. Baba, K. Demichi, Z. Fulop, J. Gibelin, T. Gomi, H. Hasegawa, N. Imai, M. Ishihara, H. Iwasaki, S. Kanno, S. Kawai, T. Kishida, T. Kubo, K. Kurita, Y. Matsuyama, S. Michimasa *et al.*, *Phys. Rev. Lett.* **96**, 182501 (2006).
- [9] J. R. Terry, D. Bazin, B. A. Brown, C. M. Campbell, J. A. Church, J. M. Cook, A. D. Davies, D.-C. Dinca, J. Enders, A. Gade, T. Glasmacher, P. G. Hansen, J. L. Lecouey, T. Otsuka, B. Pritychenko, B. M. Sherrill, J. A. Tostevin, Y. Utsuno, K. Yoneda, and H. Zwahlen, *Phys. Lett. B* **640**, 86 (2006).
- [10] S. M. Brown, W. N. Catford, J. S. Thomas, B. Fernandez-Dominguez, N. A. Orr, M. Labiche, M. Rejmund, N. L. Achouri, H. Al Falou, N. I. Ashwood, D. Beaumel, Y. Blumenfeld, B. A. Brown, R. Chapman, M. Chartier, N. Curtis, G. de France, N. de Sereville, F. Delaunay, A. Drouart *et al.*, *Phys. Rev. C* **85**, 011302(R) (2012).
- [11] H. N. Liu, J. Lee, P. Doornenbal, H. Scheit, S. Takeuchi, N. Aoi, K. A. Li, M. Matsushita, D. Steppenbeck, H. Wang, H. Baba, E. Ideguchi, N. Kobayashi, Y. Kondo, G. Lee, S. Michimasa, T. Motobayashi, A. Poves, H. Sakurai, M. Takechi *et al.*, *Phys. Lett. B* **767**, 58 (2017).
- [12] M. Holl, S. Lindberg, A. Heinz, Y. Kondo, T. Nakamura, J. A. Tostevin, H. Wang, T. Nilsson, N. L. Achouri, H. Al Falou, L. Atar, T. Aumann, H. Baba, K. Boretzky, C. Caesar, D. Calvet, H. Chae, N. Chiga, A. Corsi, H. L. Crawford *et al.* (SAMURAI21 Collaboration), *Phys. Rev. C* **105**, 034301 (2022).
- [13] H. Wang, M. Yasuda, Y. Kondo, T. Nakamura, J. A. Tostevin, K. Ogata, T. Otsuka, A. Poves, N. Shimizu, K. Yoshida, N. L. Achouri, H. Al Falou, L. Atar, T. Aumann, H. Baba, K. Boretzky, C. Caesar, D. Calvet, H. Chae, N. Chiga *et al.*, *Phys. Lett. B* **843**, 138038 (2023).
- [14] H. Iwasaki, T. Motobayashi, H. Sakurai, K. Yoneda, T. Gomi, N. Aoi, N. Fukuda, Zs. Fülöp, U. Futakami, Z. Gacsi, Y. Higurashi, N. Imai, N. Iwasa, T. Kubo, M. Kunibu, M. Kurokawa, Z. Liu, T. Minemura, A. Saito, M. Serata *et al.*, *Phys. Lett. B* **620**, 118 (2005).
- [15] A. Obertelli, A. Gillibert, N. Alamanos, M. Alvarez, F. Auger, R. Dayras, A. Drouart, G. de France, B. Jurado, N. Keeley, V. Lapoux, W. Mittig, X. Mougeot, L. Nalpas, A. Pakou, N. Patronis, E. C. Pollacco, F. Rejmund, M. Rejmund, P. Roussel-Chomaz *et al.*, *Phys. Lett. B* **633**, 33 (2006).
- [16] N. Kobayashi, T. Nakamura, Y. Kondo, J. A. Tostevin, N. Aoi, H. Baba, R. Barthelemy, M. A. Famiano, N. Fukuda, N. Inabe, M. Ishihara, R. Kanungo, S. Kim, T. Kubo, G. S. Lee, H. S. Lee, M. Matsushita, T. Motobayashi, T. Ohnishi, N. A. Orr *et al.*, *Phys. Rev. C* **93**, 014613 (2016).
- [17] A. Revel, J. Wu, H. Iwasaki, J. Ash, D. Bazin, B. A. Brown, J. Chen, R. Elder, P. Farris, A. Gade, M. Grinder, N. Kobayashi, J. Li, B. Longfellow, T. Mijatovic, J. Pereira, A. Poves, A. Sanchez, N. Shimizu, M. Spieker *et al.*, *Phys. Lett. B* **838**, 137704 (2023).
- [18] P. Doornenbal, H. Scheit, S. Takeuchi, Y. Utsuno, N. Aoi, K. Li, M. Matsushita, D. Steppenbeck, H. Wang, H. Baba, E. Ideguchi, N. Kobayashi, Y. Kondo, J. Lee, S. Michimasa, T. Motobayashi, T. Otsuka, H. Sakurai, M. Takechi, Y. Togano *et al.*, *Phys. Rev. C* **95**, 041301(R) (2017).
- [19] S. Bagchi, R. Kanungo, Y. K. Tanaka, H. Geissel, P. Doornenbal, W. Horiuchi, G. Hagen, T. Suzuki, N. Tsunoda, D. S. Ahn, H. Baba, K. Behr, F. Browne, S. Chen, M. L. Cortes, A. Estrade, N. Fukuda, M. Holl, K. Itahashi, N. Iwasa *et al.*, *Phys. Rev. Lett.* **124**, 222504 (2020).
- [20] A. Revel, O. Sorlin, F. M. Marqués, Y. Kondo, J. Kahlbow, T. Nakamura, N. A. Orr, F. Nowacki, J. A. Tostevin, C. X. Yuan, N. L. Achouri, H. Al Falou, L. Atar, T. Aumann, H. Baba, K. Boretzky, C. Caesar, D. Calvet, H. Chae, N. Chiga *et al.* (SAMURAI21 collaboration), *Phys. Rev. Lett.* **124**, 152502 (2020).
- [21] T. L. Tang, T. Uesaka, S. Kawase, D. Beaumel, M. Dozono, T. Fujii, N. Fukuda, T. Fukunaga, A. Galindo-Uribarri, S. H. Hwang, N. Inabe, D. Kameda, T. Kawahara, W. Kim, K. Kisamori, M. Kobayashi, T. Kubo, Y. Kubota, K. Kusaka, C. S. Lee *et al.*, *Phys. Rev. Lett.* **124**, 212502 (2020).
- [22] H. L. Crawford, M. D. Jones, A. O. Macchiavelli, P. Fallon, D. Bazin, P. C. Bender, B. A. Brown, C. M. Campbell, R. M. Clark, M. Cromaz, B. Elman, A. Gade, J. D. Holt, R. V. F. Janssens, I. Y. Lee, B. Longfellow, S. Paschalis, M. Petri, A. L. Richard, M. Salathe *et al.*, *Phys. Rev. C* **106**, L061303 (2022).
- [23] D. Guillemaud-Mueller, J. C. Jacmart, E. Kashy, A. Latimier, A. C. Mueller, F. Pougheon, A. Richard, Y. E. Penionzhkevich, A. G. Artuhk, A. V. Belozyorov, S. M. Lukyanov, R. Anne, P. Bricault, C. Détraz, M. Lewitowicz, Y. Zhang, Y. S. Lyutostansky, M. V. Zverev, D. Bazin, and W. D. Schmidt-Ott, *Phys. Rev. C* **41**, 937 (1990).
- [24] E. Lunderberg, P. A. DeYoung, Z. Kohley, H. Attanayake, T. Baumann, D. Bazin, G. Christian, D. Divaratne, S. M. Grimes, A. Haagsma, J. E. Finck, N. Frank, B. Luther, S. Mosby, T. Nagi, G. F. Peaslee, A. Schiller, J. Snyder, A. Spyrou, M. J. Strongman *et al.*, *Phys. Rev. Lett.* **108**, 142503 (2012).
- [25] Z. Kohley, T. Baumann, D. Bazin, G. Christian, P. A. DeYoung, J. E. Finck, N. Frank, M. Jones, E. Lunderberg, B. Luther, S. Mosby, T. Nagi, J. K. Smith, J. Snyder, A. Spyrou, and M. Thoennessen, *Phys. Rev. Lett.* **110**, 152501 (2013).

- [26] C. Caesar, J. Simonis, T. Adachi, Y. Aksyutina, J. Alcantara, S. Altstadt, H. Alvarez-Pol, N. Ashwood, T. Aumann, V. Avdeichikov, M. Barr, S. Beceiro, D. Bemmerer, J. Benlliure, C. A. Bertulani, K. Boretzky, M. J. G. Borge, G. Burgunder, M. Caamano, E. Casarejos *et al.* (R3B Collaboration), *Phys. Rev. C* **88**, 034313 (2013).
- [27] Y. Kondo, T. Nakamura, R. Tanaka, R. Minakata, S. Ogoshi, N. A. Orr, N. L. Achouri, T. Aumann, H. Baba, F. Delaunay, P. Doornenbal, N. Fukuda, J. Gibelin, J. W. Hwang, N. Inabe, T. Isobe, D. Kameda, D. Kanno, S. Kim, N. Kobayashi *et al.*, *Phys. Rev. Lett.* **116**, 102503 (2016).
- [28] F. Marti, P. Miller, D. Poe, M. Steiner, J. Stetson, and X. Y. Wu, *AIP Conf. Proc.* **600**, 64 (2001).
- [29] D. Morrissey, B. M. Sherrill, M. Steiner, A. Stolz, and I. Wiedenhoever, *Nucl. Instrum. Methods Phys. Res. B* **204**, 90 (2003), 14th International Conference on Electromagnetic Isotope Separators and Techniques Related to their Applications.
- [30] T. Redpath, T. Baumann, J. Brown, D. Chrisman, P. A. DeYoung, N. Frank, P. Guèye, A. N. Kuchera, H. Liu, C. Persch, S. Stephenson, K. Stiefel, M. Thoennessen, and D. Votaw, *Nucl. Instrum. Methods Phys. Res. A* **977**, 164284 (2020).
- [31] M. D. Bird, S. J. Kenney, J. Toth, H. W. Weijers, J. C. DeKamp, M. Thoennessen, and A. F. Zeller, *IEEE Trans. Appl. Supercond.* **15**, 1252 (2005).
- [32] T. Baumann, J. Boike, J. Brown, M. Bullinger, J. P. Bychoswki, S. Clark, K. Daum, P. A. DeYoung, J. V. Evans, J. Finck, N. Frank, A. Grant, J. Hinnefeld, G. W. Hitt, R. H. Howes, B. Isselhardt, K. W. Kemper, J. Longacre, Y. Lu, B. Luther *et al.*, *Nucl. Instrum. Methods Phys. Res. A* **543**, 517 (2005).
- [33] T. Redpath, Measuring the half-life of O-26, Ph.D. thesis, Michigan State University, 2019.
- [34] G. A. Christian, Production of nuclei in neutron unbound states via primary fragmentation of ^{48}Ca , Master's thesis, Michigan State University, 2008.
- [35] Z. Kohley, E. Lunderberg, P. A. DeYoung, B. T. Roeder, T. Baumann, G. Christian, S. Mosby, J. Smith, J. Snyder, A. Spyrou, and M. Thoennessen, *Nucl. Instrum. Methods Phys. Res. A* **682**, 59 (2012).
- [36] K. Fosseze, J. Rotureau, N. Michel, and W. Nazarewicz, *Phys. Rev. C* **96**, 024308 (2017).
- [37] Y. Kondo, private communication (2023).
- [38] M. Thoennessen, T. Baumann, B. A. Brown, J. Enders, N. Frank, P. G. Hansen, P. Heckman, B. A. Luther, J. Seitz, A. Stolz, and E. Tryggestad, *Phys. Rev. C* **68**, 044318 (2003).
- [39] A. Schiller, N. Frank, T. Baumann, D. Bazin, B. A. Brown, J. Brown, P. A. DeYoung, J. E. Finck, A. Gade, J. Hinnefeld, R. Howes, J.-L. Lecouey, B. Luther, W. A. Peters, H. Scheit, M. Thoennessen, and J. A. Tostevin, *Phys. Rev. Lett.* **99**, 112501 (2007).
- [40] R. S. Lubna, K. Kravvaris, S. L. Tabor, V. Tripathi, E. Rubino, and A. Volya, *Phys. Rev. Res.* **2**, 043342 (2020).
- [41] B. A. Brown, *Physics* **4**, 525 (2022).
- [42] P. G. Hansen and J. A. Tostevin, *Annu. Rev. Nucl. Part. Sci.* **53**, 219 (2003).
- [43] J. A. Tostevin and B. A. Brown, *Phys. Rev. C* **74**, 064604 (2006).
- [44] J. A. Tostevin and A. Gade, *Phys. Rev. C* **103**, 054610 (2021).
- [45] M. D. Jones, K. Fosseze, T. Baumann, P. A. DeYoung, J. E. Finck, N. Frank, A. N. Kuchera, N. Michel, W. Nazarewicz, J. Rotureau, J. K. Smith, S. L. Stephenson, K. Stiefel, M. Thoennessen, and R. G. T. Zegers, *Phys. Rev. C* **96**, 054322 (2017).